Hematopoietic Stem Cell Gene Therapy Alleviates Disease Phenotypes in a Murine Model of Danon Disease

Chao Chen
University of California, San Diego
Sherin I. Hashem
University of California, San Diego
Jay Sharma
University of California, San Diego
Ana Maria Manso
University of California, San Diego
Paul Bushway
University of California, San Diego
Jason M. Duran
University of California, San Diego
Emily C. Gault
University of California, San Diego
Yusu Gu
University of California, San Diego
Jose Roberto Cano Nigenda
University of California, San Diego
Angel Soto-Hermida
University of California, San Diego
Kirk L. Peterson
University of California, San Diego
Paul Saftig
Biochemisches Institut, Christian Albrecht Universität Kiel, Kiel, Germany https://orcid.org/0000-0003-2637-7052
Sylvia M. Evans
University of California San Diego
Stephanie Cherqui
University of California, San Diego
Eric D. Adler (eradler@ucsd.edu)
University of California, San Diego

Article

Keywords: Danon disease, Autophagy, Hematopoietic Stem and Progenitor Cells, Lentiviral vector, Gene Therapy, Lysosomal associated membrane protein type 2 (LAMP2), Cardiovascular Disease

Posted Date: August 19th, 2022

DOI: https://doi.org/10.21203/rs.3.rs-1921280/v1

Abstract

Danon disease is a fatal X-linked recessive disease caused by a lack of expression of the lysosomal associated membrane protein type 2 (LAMP2), leading to severe vacuolar cardiomyopathy. Most patients with Danon progress to end-stage heart failure or death without advanced therapies. In this study, we investigated the therapeutic efficacy of systemic transplantation of *ex vivo* gene-modified *Lamp2*$^{-/-}$ (*Lamp2* KO) hematopoietic stem and progenitor cells (HSPCs) using a lentiviral vector containing the human LAMP2B transgene, pCCL-LAMP2B, in the mouse model of Danon disease, *Lamp2* KO mice. Transplanted pCCL-LAMP2B-HSPCs efficiently engrafted and differentiated into macrophages in heart. LAMP2B was found in cardiomyocytes and improved cardiac systolic as well as locomotor functions were observed in pCCL-LAMP2B-HSPCs recipient mice compared to non-treated or *Lamp2* KO mice receiving *Lamp2* KO HSPCs. In addition, we also demonstrated that pCCL-LAMP2B-HSPCs rescued autophagic flux and activity in the heart. *In vitro*, we cocultured WT macrophages with *Lamp2* KO fibroblasts and observed transfer of LAMP2B and rescue of the autophagic flux in the diseased cells confirming cross-correction despite LAMP2B being a lysosomal transmembrane protein.

Introduction

Danon disease is a fatal condition associated with profound cardiac and skeletal vacuolar myopathies. Without heart transplant, patients progress to end-stage heart failure and die during the second or third decade of life[1, 2]. Danon is caused by mutations in Lysosomal Associated Membrane Protein type-2 (LAMP2), a highly glycosylated lysosomal membrane-bound protein that is an important component of lysosome membrane function and autophagosome-lysosome fusion [3, 4]. The lack of functional LAMP2 protein is associated with an extensive accumulation of autophagic vacuoles in many tissues, particularly skeletal and heart muscle (the hallmark of Danon disease).

Our group previously demonstrated that simultaneous long-term rescue of various tissues could be achieved through the hematopoietic stem and progenitor cell (HSPC) transplantation using another multi-systemic disease model belonging to the lysosomal storage disorders, cystinosis[5, 6, 7, 8], for which the protein involved is also a transmembrane lysosomal protein[9, 10]. We showed that the mechanism underlying this therapeutic effect involves the differentiation of HSPC into tissue-resident phagocytic cells that provide “healthy lysosomes” carrying the functional protein cystinosin to the host disease cells via Tunneling Nanotubes (TNTs). TNTs contain microtubules that allow migration of organelles such as lysosomes[11, 12]. This method of using lentivirus-modified autologous HSPC gene therapy for cystinosis[13] has led to an ongoing phase 1/2 clinical trial at the University of California San Diego (ClinicalTrials.gov Identifier: NCT03897361). We hypothesize that a similar strategy using lentivirus-modified autologous HSPC *ex vivo* gene therapy could be used to treat other lysosomal storage disorders including Danon disease.

Several studies have used adeno-associated viruses (AAVs) as a gene therapy delivery system to target specific tissues such as skeletal muscles, lung, liver, and eye[14, 15] We previously demonstrated that

expression of exogenous LAMP2B by systemic AAV9.LAMP2B injection reversed metabolic and physiologic multiorgan dysfunction in a murine model of Danon disease. Although these results are promising, safety issues have been raised relating to liver toxicity and organ failure resulting from high viral dosages[16]. High viral titers are often required to achieve therapeutic benefit in patients due to inefficiencies in systemic viral administration driving up production costs that directly impact the cost of therapy. Furthermore, AAV therapies are not a therapeutic option for individuals who harbor natural immunity to the AAV capsid. Thus, we evaluated the therapeutic potential of HSPC transplantation (both WT HSPC and gene-modified *Lamp2* KO HSPC) in the context of Danon disease using *in vitro* and *in vivo* models.

Materials And Methods

Mice

C57BL/6 *Lamp2* knockout (KO) mice were provided by the laboratory of Dr. Paul Saftig[17] and bred continuously at the University of California San Diego (UCSD). Transgenic mice constitutively expressing CAG-RFP-EGFP-LC3B (tLC3) were provided by Dr. Joseph Hill (UT Southwestern) [18] and were crossed with C57BL/6 *Lamp2* KO mice[19]. Transgenic mice constitutively expressing GFP (C57BL/6-Tg [ACTB-EGFP]1Osb/J) were purchased from Jackson Laboratory (Bar Harbor, ME, USA). All protocols were approved by the UCSD Institutional Animal Care and Use Committee (IACUC).

Generation of GFP-, LAMP2- and LAMP2-GFP -Lentivirus (LVs)

The SIN-LV, pCCL-EFS-X-WPRE (pCCL) was used for gene transfer. The vector backbone is based on the pCCL-LVs [20] and contains the intron-less human elongation factor 1α promoter (242 bp) to drive transgene expression[21]. The *GFP*, human *LAMP2* cDNA, and the fusion *LAMP2-GFP* cDNA were inserted into pCCL at the *Bam*HI and *Sal*I restriction sites; they were named pCCL-GFP, pCCL-LAMP2B, and pCCL-LAMP2GFP, respectively.

Production of LVs and titers

Infectious LV particles were produced using the transient tri-transfection procedure in human embryonic kidney 293T cells. Packaging plasmids along with the expression constructs were used resulting to assemble vesicular stomatitis virus-G glycoprotein pseudotyped viral particles. Vector particles were collected in 25 ml of Stemspan medium (StemCell Technologies, Vancouver, Canada) and concentrated 100 times by ultracentrifugation at 25,000 rpm for 2 hours at 4 °C. Titers of the concentrated virus were measured by infection of 293T cells after serial dilutions of viral preparations and determined by flow cytometry for pCCL-GFP and IVIS imaging system for pCCL-LUC. Titers for pCCL-LAMP2B viral particles were measured by infection of fibroblast cells and determined by ddPCR on genomic DNA as described below. Viral titers of concentrated supernatant ranged from 6×10^8 to 8×10^8 transducing units/ml

depending on the vector. A vector rescue assay demonstrated that replication-competent lentivirus was absent in both the vector preparation media and the blood of transplanted mice.

Bone marrow cell isolation, transplantation, and engraftment assessment

Bone marrow cells were flushed from the long bones of 6- to 8-week-old GFP-transgenic WT or *Lamp2* KO mice. Sca-1 positive (Sca-1$^+$) HSPCs were isolated by immunomagnetic separation using anti-Sca-1 antibody conjugated to magnetic beads (Miltenyi Biotec) as previously described[11]. After 24 hours cells transduced with or without pCCL-LAMP2B were directly transplanted by tail vein injection in lethally irradiated (7 or 10 gray; X-Rad 320, PXi) 8-10-week-old *Lamp2* KO mice at a concentration of one million Sca-1/GFP-positive cells suspended in 100 µl of phosphate-buffered saline (PBS). Bone marrow engraftment of the transplanted cells was assessed by flow cytometry of fresh peripheral blood at 2-months post-transplantation. Fresh peripheral blood was lysed in red blood cell lysis buffer (eBioscience, San Diego, CA, USA) and subsequently ddPCR analyzed by flow cytometry to quantify the proportion of GFP-positive (GFP$^+$) cells for the WTHSPC engraftment.

Cardiac catheterization

Invasive hemodynamics were performed under general anesthesia (ketamine (100 mg kg)/xylazine (10 mg/kg)) after intubation and ventilation. A 1.4 french (0.46 mm) micromanometer catheter (Millar Instruments) was inserted (via the common carotid artery) into the ascending aorta, and then across the aortic valve into the LV; phasic and mean pressures were continuously monitored using a LabChart (AD Instruments®, Australia) system. Digital post-processing of micromanometer pressure signal, for calculation of maximum and minimum derivative of pressure over time (max or min dP/dT) was performed as previously described[22].

Neurobehavioral study

Littermate wild-type (WT) mice, *Lamp2 KO* mice, WT GFP transplanted *Lamp2 KO* mice and pCCL-LAMP2B HSPC transplanted mice underwent neurobehavioral testing before being sacrificed for tissue analysis. Open-field locomotor activity was performed by using an automated monitoring system (Kinder Associates)[23]. Polycarbonate cages (42 × 22 × 20 cm) containing a thin layer of bedding material were placed into frames (25.5 × 47 cm) mounted with photocell beams. Each mouse was placed into the open field, and all movements were recorded over a 20 min period. The total path length, the immobile time, the mean speed as well as the time stayed in different areas were measured.

Blood Chemistry for metabolic panel

Blood was collected via abdominal venipuncture and serum was collected after a 1-minute centrifuge at 13,000 rpm. Comprehensive diagnostic profiling #500-0038 using Abaxis Vet Scan portfolio was conducted on serum samples for each mouse at study termination at the UCSD ACP veterinary diagnostic lab.

Annexin V FITC and PI assay for dead cell staining

Cells at a concentration of 0.5 × 10^6 per sample were stained with CD34-PE and CD45-APC/Cy7 (allophycocyanin, BD Biosciences, San Jose, CA, USA) antibodies in a round-bottom tube (BD Falcon) and incubated for 15 minutes at room temperature in the dark. Cells were incubated in 2 mL Lyse buffer for 10 minutes (4°C), samples were centrifuged for 7 min (500 g, 4°C) and resuspended in 500 µL Annexin V binding buffer (BD Pharmingen). Annexin V-FITC (BD Pharmingen, CA, USA) and 7-AAD were added and incubated for at least 10 minutes at room temperature before flow cytometric measurement was performed. Viable cells (FITC-/PI-), apoptotic cells ($FITC^+/PI^-$), and necrotic cells ($FITC^+/PI^+$) were quantified by Flow cytometry.

Reverse transcription and qPCR

RNA was isolated by RNeasy Kits (Qiagen, Germantown, MD, USA) then 1µg RNA was reverse transcribed using iScript cDNA Synthesis Kit (Bio-Rad, Hercules, CA). qPCR was performed using either 2µl of cDNA or 200ng of genomic DNA with 2x Applied Biosystems™ SYBR™ Green master mix using an Applied Biosystems 7900 HT (Applied Biosystems, Waltham, MA). Primers and probes were obtained from Applied Biosystems.

Mouse specific lamp2 primer:

mLAMP2-F:GAGCAGGTGCTTTCTGTGTCTAG
mLAMP2-R: GCCTGAAAGACCAGCACCAACT

Human specific lamp2 primer:

Hulamp2-F: GTGCAACAAAGAGCAGACTG

Hulamp2-R: TACAGAGTCTGATATCCAGCATAAC

GAPDH primer:

GAPDH-F:CACAGTCAAGGCCGAGAATGGGAA

GAPDH-R:GTGGTTCACACCCATCACAAACATG

Vector Copy Number determination

Lentiviral integration site patterns were detected on genomic DNA from blood and spleen as previously described[24]. Briefly, high-quality genomic DNA (gDNA) was extracted using QuickExtract (Lucigen, Middleton, WI, USA) and from tissues using a DNeasy Blood & Tissue kit (QIAGEN, Germantown, MD, USA). To measure the efficiency, 100 ng of gDNA, HindIII (NEB, Ipswich, MA, USA), and 1× digital droplet PCR (ddPCR) supermix for probes (no dUTP [deoxyuridine triphosphate]) (Bio-Rad, Hercules, CA, USA) were used in combination with two sets of primers/probes to generate the droplets using the QX200

droplet generator (Bio-Rad, Hercules, CA, USA). Next, the droplets were transferred to a 96-well plate and the following PCR was carried out: 95°C for a 10-min ramp at 2°C/s, (94°C for 30-s ramp at 2°C/s, 60°C for a 1-min ramp at 2°C/s) × 39, 98°C for 10-min ramp at 2°C/s. The 96-well plate was then read by the QX200 Droplet Reader (Bio-Rad, Hercules, CA, USA).

pCCL vector primer:

Fwd Primer: ACTTGAAAGCGAAAGGGAAAC

Rev Primer: CGCACCCATCTCTCTCCTTCT

Co-culture experiments and imaging

Primary fibroblasts were derived from skin biopsies of neonatal *Lamp2* KO/CAG-RFP-EGFP-LC3B mice and maintained in high-glucose Dulbecco's modified Eagle's medium (DMEM, (Gibco Life Technologies, Paisley, UK) supplemented with 10% fetal bovine serum (FBS; Gibco Life Technologies) and 1% penicillin/streptomycin (P/S; Gibco Life Technologies) at 37°C under 5% CO_2. IC-21 macrophage cell line (American Type Culture Collection #TIB-186) were cultured in medium containing RPMI 1640, 10% FBS, and 1% P/S at 37°C under 5% CO_2. For co-culture experiments, IC-21 macrophages were co-cultured with fibroblasts derived from *Lamp2* KO/CAG-RFP-EGFP-LC3B-mice at a ratio of 1:1 and plated at a density of 1500 cells per coverslip in 300 ml of medium containing high-glucose DMEM, 10% FBS, and 1% P/S at 37°C under 5% CO2 for 72 hrs. Images were captured, processed, and analyzed using a Nikon C2 confocal microscope.

Electron microscopy (EM) and autophagic vacuole quantification:

Mouse hearts were fixed and embedded using standard operating procedures for EM. Briefly, cardiac tissue was infused with 2.3 M sucrose for 1 hour, mounted on silver pins, and frozen in liquid nitrogen. Ultrathin cryosections were cut at -110°C on a Leica Ultracut (Wetzlar, Germany), collected in a 1:1 mixture of 2% methylcellulose and 2.3 M sucrose, transferred to Formvar/carbon-coated grids, and embedded in 2% methylcellulose, 0.4% uranyl acetate. Sections were imaged at 60-80kV in a JEOL 1230 electron microscope and recorded with a Morada digital camera using iTEM (SIS) software. More than 10 fields were scored per mouse. Only cardiac muscle cells were assessed. Quantitative data are presented as the average values collected for each study group.

Immunofluorescence and image acquisition

Heart tissues were fixed in 4% paraformaldehyde overnight at 4°C, equilibrated in 30% sucrose overnight, frozen in Tissue-Tek optimal cutting temperature (OCT) medium at −80°C (Sakura Finetek USA), and sectioned into 10-μm sections using a Leica CM3050S cryotome (Wetzlar, Germany). For immunofluorescence, tissues were incubated with the following antibodies: Rat anti-mouse LAMP2 (ABL-93) and Mouse anti-Mouse monoclonal LAMP2/CD107b (H4B4) Alexa Fluor 647 (Novus Biologicals); rabbit anti-sarcomeric a-actinin (EP2529Y, GeneTex), rat anti-CD68 (137001, BioLegend), Dystrophin

(Sigma), Rat anti-mouse LAMP2 antibody (Abl 93; Developmental Studies Hybridoma Bank), DAPI (Molecular Probes). The appropriate Alexa Fluor–conjugated secondary antibodies (Invitrogen) were used for the visualization of antigens. Images were acquired using an Olympus FluoView^{TM} FV1000 (Olympus GmbH, Hamburg, Germany) and Zeiss LSM 880 Confocal with FAST Airyscan microscope (Oberkochen, Germany). Adobe Photoshop 2020 and Zeiss Zen were used to analyze the images. Alexa Fluor 488 goat anti-rabbit, (A-11029) and DAPI (all from Molecular Probes, Invitrogen),

Western Blot

Whole-cell lysates (20 µg) were resolved on 4-20% SDS-PAGE denaturing gels and transferred to PVDF nylon membranes. Membranes were blocked with 5% non-fat dry milk in TBST and probed with anti-LAMP2 (Abl 93; Developmental Studies Hybridoma Bank, 1:250; Iowa City, IA) or anti-LC3B (L7543, Sigma), human LAMP2 (H4B4) (Developmental Studies Hybridoma Bank); Rabbit anti-LC3B (Sigma), primary antibodies overnight at 4^0C, and re-probed with anti-GAPDH (GTX 100118, GeneTex) or GAPDH (Santa Cruz Biotechnology) as a loading standard. Quantification was performed using ImageJ, and data is presented as the average of LC3-II/GAPDH or LAMP2/GAPDH values collected.

Statistics: Differences between means of two or more experimental groups were determined by one Way *ANOVA* by GraphPad Prism 8.0. Values are expressed as means ± standard error of the mean (SEM). A p-value of ≤ 0.05 was considered statistically significant. All results were presented in Scatter plots or Column bar graphs created by GraphPad Prism 8.0.

Results

WT and pCCL-LAMP2B-HSPC transplantation improved survival in *Lamp2* KO mice with efficient engraftment

Two-month-old *Lamp2* KO mice were lethally irradiated and infused with Sca1$^+$ *Lamp2* KO HSPC *ex vivo* transduced with pCCL-LAMP2B (n=24). As controls, Lamp2 mice were transplanted with pCCL-GFP(N=5), WT GFP$^+$ HSPCs (n=28) or *Lamp2* KO HSPCs (n=28); WT littermates were used as the physiologic baseline for all the experiments. To investigate engraftment, peripheral blood samples were analyzed at 2 months post-transplantation. An average of 62.42 ± 13.91% of WT HSPC cells were GFP$^+$ *vs.* 77.29 ± 13.06% of the *Lamp2* KO HSPC transplanted mice (Fig. 1C) as assessed by flow cytometry. Analysis of viral copy number (VCN) in blood of the LAMP2 transduced group showed a range from 0.31 to 3.24. Compete Blood Count (CBC) was evaluated after HSPC transplantation to assess blood cell reconstitution and showed no difference between groups (Supplemental Table 1).

When experiments were terminated at 6 months post transplantation, survival of the mice varied between the different groups: 23 of 28 WT HSPCs mice (Survival ratio 82.1%), 14 of 24 pCCL-LAMP2B HSPC (Survival ratio 58.3%), 6 of 28 KO HSPC mice (Survival ratio 21.4%) and 0 of 5 pCCL-GFP HSPC (Survival

ratio 0%). Body weight, liver weight, or heart weight were weighed and showed no difference post the irradiation and transplantation(Fig S3 A-C), however, spleen weight was significantly heavier in the KO group (185±9.1mg) compared with the WT group (82.4±6.1 mg). After the pCCL-LAMP2 HSPC transplantation, spleen weight reduced from 185.4±9.13 mg in KO HSPC to 78.84±5.1 mg in pCCL-LAMP2 HSPC, and 69.84±7.1 mg in WT HSPC (Fig S3 D).

These data indicated that the mice in pCCL-LAMP2B HSPC and WT HSPC groups showed increased survival and reduced spleen weight compared with KO HSPC or pCCL-GFP HSPC groups.

pCCL-LAMP2B HSPC transplantation improved the cardiac systolic function in Danon disease mice by inducing de novo-expression of LAMP2B and rescuing cardiomyocyte autophagic flux

We previously demonstrated a reduction in cardiac contractile function by invasive hemodynamic studies in LAMP2 KO Mice [22]. Hence, we performed invasive hemodynamic studies on the mice at 6 months post-transplantation. Cardiac contraction and relaxation as evaluated by dP/dt max, dP/dt min (positive and negative first derivatives for maximal rates of left ventricular pressure development, respectively), and Tau (left ventricular relaxation time constant) were measured. Since all the transplanted mice went through a lethal dose of irradiation, the KO HSPC group was used as a control.

Interestingly, pCCL-LAMP2B significantly improved cardiac systolic function measured by max dP/dT versus the KO HSPC transplanted group (Fig.2A-2D) (5650 ± 719.4 v. 2923 ± 414.2 mmHg/s in pCCL-LAMP2B vs. KO HSPC; p= 0.0434). These data demonstrate that pCCL-LAMP2B HSPC transplantation improved cardiac contractile dysfunction in the Danon mouse model.

VCNs in heart tissue ranged from 0.02 to 0.5 in pCCL-LAMP2B HSPC treated mice(Fig. 2E). HuLAMP2 expression was measured using Western blot analysis and revealed that HuLAMP2 was expressed in a blood VCN-dependent fashion in total cardiac tissue lysates (Figure 2F), and LC3 levels decreased accordingly. Similarly, murine Lamp2 expression increased with decreased LC3 expression in cardiac lysates from WT HSPC-treated mice. To prove that HuLAMP2 or MuLAMP2 were expressed specifically in cardiomyocytes, western blot analysis was performed on isolated adult ventricular cardiomyocytes. HuLAMP2 was expressed in cardiomyocytes isolated from pCCL-LAMP2B HSPC transplanted mice and MuLAMP2 was expressed in cardiomyocytes isolated from WTGFP transplanted mice. LC3 reduction was also observed in concert with the de novo expression of LAMP2, which suggested that autophagic flux improved with expression of LAMP2 in cardiomyocytes.

Next, we investigated whether successful de novo expression of LAMP2 protein in *Lamp2*KO mice would rescue the pathogenesis the hallmark of in Danon disease: autophagic vacuolization. Fixed heart

sections from WT, KO, pCCL-LAMP2B HSPC, WT HSPC, and KO HSPC transplanted *Lamp2* KO mice were assessed for vacuolization using electron microscopy. We noted a significant reduction in the number of autophagic vacuoles within cardiomyocytes of pCCL-LAMP2B HSPC, WT HSPC compared to non-transplanted *Lamp2* KO mice (Fig.2J). Hence, both molecular and EM analysis suggest that HSPC transplantation restores LAMP2 expression and rescued autophagic flux in a mouse model of Danon disease in vivo.

Together, these data indicated that pCCL-LAMP2B HSPC transplantation improved cardiac metabolic and physiologic function in a Danon mouse model at 6 months post-transplantation.

pCCL-LAMP2B HSPC and WT HSPC transplantation improved abnormal behavior seen in the Danon disease mouse model in an Open Field Maze study

Intellectual disabilities, abnormal behavior, motor deficits and impaired learning have been widely reported in human Danon patients, and neuropathological changes including cerebral inflammation have been described in prior mouse models and human autopsy studies[25]. We tested the impact of pCCL-LAMP2B and WT HSPCs on the behavior of the *Lamp2* KO mouse using the Open-field Maze. The walking distance of both the pCCL-LAMP2B HSPC (85.85 ± 14.97 m) and WT HSPC (64.9 ± 18.09 m) groups was significant longer than the KO HSPC (50.4 ± 17.04m) group (Fig. 3A), and walking speed were also faster (pCCL-LAMP2B HSPC 0.057±0.01m/s *vs*. WT HSPC 0.043 ± 0.012 m/s *vs*. KO HSPC 0.033± 0.011 m/s) (Fig. 3B); the immobile time during exploration of a novel environment improved as well (pCCL-LAMP2B HSPC 157± 83.57s *vs*. HSPC WT HSPC 265.7 ±90.3s *vs*. KO 446± 81s;) (Fig. 3C). VCN and LAMP2 protein expression were observed in brain and skeletal muscle with an associated decrease in LC3-II levels (Fig.3 D and E).

These data indicate that pCCL-LAMP2B HSPC transplantation improves locomotor function with LAPM2B de novo expression in brain and muscle of Danon mice at 6 months post -transplantation.

Donor HSPCs differentiate into phagocytic cells in target tissues and transfer LAMP2B protein to diseased cardiomyocytes in *Lamp*2 KO mice.

Given that heart is the primary affected organ in Danon disease, with severe cardiac fibrosis, we hypothesized that hearts of *Lamp2* KO mice would exhibit an increase in tissue histiocytes (macrophages) secondary to cell injury. To test this hypothesis, WT and *Lamp2* KO mouse hearts underwent immunohistochemical analysis for the presence of $CD68^+$ macrophages. As expected, there was an increase in $CD68^+$ cells in hearts of *Lamp2* KO mice compared to age-matched WT controls (number of macrophages/600x field is 3.1±1.6 vs. 14.8±5.3 in 8-month-old WT vs. *Lamp2* KO mouse hearts; $p<0.05$; Supplemental Fig. S2). *Lamp2* KO mouse hearts harbored an increased number of $CD68^+$

macrophages as compared to control littermates, possibly due to increased tissue injury in Danon disease hearts. These data suggested that inflammation plays a key role in recruitment and engraftment of bone marrow HSPCs in target tissues.

HSPC-derived cells within hearts of WT GFP^+ HSPC-transplanted mice were then characterized at 6 months post-transplantation. Donor-derived GFP^+ cells were observed in the mouse hearts of HSPC-transplanted mice 6 months post-transplantation (Fig. 4A-C), showing that a single GFP^+ HSPC infusion was sufficient for long-term, widespread, and durable integration of donor HSPC cells into recipient myocardium. Immunofluorescent counterstaining demonstrated that engrafted HSPC-derived GFP^+ cells were also $CD68^{+,}$ indicating that donor HSPCs differentiated into macrophages within hearts of the $Lamp2^{-/-}$ mice (Fig.4A-E). $GFP^+/CD68^+$ macrophages showed diffuse spatial distribution throughout the myocardium allowing for widespread direct contact between the donor-derived macrophages and the *Lamp2* KO recipient cardiac myocytes. In WT-HSPC transplanted *Lamp2* KO mice, $LAMP2^+$ vesicles were identified within sarcomeric α-actinin$^+$ cardiomyocytes that were located adjacent to donor-derived GFP^+ cells, suggesting the transfer of $LAMP2^+$ lysosomes from engrafted WT-HSPC-derived macrophages into *Lamp2* deficient cardiomyocytes. Similarly, we observed co-expression of CD68 and LAMP2B in the heart and in cardiomyocytes in mice transplanted with pCCL-LAMP2B HSPCs (Fig.4 D and E). LAMP2 was absent from the *Lamp2* KO cardiomyocytes.

These data demonstrate that donor HSPCs differentiated into macrophages within the heart and transferred LAMP2 protein to deficient cardiomyocytes in Danon mice.

Co-culture with wild-type macrophages rescues autophagic flux in diseased *Lamp2* KO mouse fibroblasts by transfer of LAMP2

A co-culture system with wild-type macrophages and KO fibroblasts containing an autophagic flux sensor was developed to verify that macrophages derived from transplanted HSPCs transfer LAMP2 to diseased cells. We previously reported the generation of a *Lamp2* KO line crossed with a tandem CAG-RFP-EGFP-LC3B (tLC3) line to monitor and assess autophagic flux in a mouse model of Danon disease[18, 26]. The tLC3 reporter allows for monitoring of autophagosome-lysosome fusion. In this reporter model, early autophagosomes (not fused with lysosomes) exhibit both RFP and eGFP fluorescence ($RFP^+/eGFP^+$); while late autolysosomes (autophagosomes fused with lysosomes) emit only RFP fluorescence because the eGFP emission is quenched by the acidic environment inside the lysosomes ($RFP^+/eGFP^-$). *Lamp2* KO/tLC3 cardiomyocytes exhibited an increase of overall autophagic vacuoles (AVs), an accumulation of $RFP^+/eGFP^+$ early autophagosomes (Fig.5C, yellow puncta), and were nearly devoid of $RFP^+/eGFP^-$ late autolysosomes (Fig.5D *vs.* 5K, red puncta). The absence of $RFP^+/eGFP^-$ puncta (Fig.5D) suggests that LAMP2 deficiency impairs the fusion of autophagosomes and lysosomes resulting in the accumulation of $RFP^+/EGFP^+$ autophagosomes[19]. To test the tLC3 sensor, primary mouse fibroblasts derived from

C57BL/6 *Lamp2* KO/tLC3 were cocultured with a well-established WT macrophage cell line (C57BL/6 IC-21 cells) (Fig. 5). After a 72hrs, Lamp2$^+$ puncta in the *Lamp2* KO/tLC3 fibroblasts were observed in the proximity of macrophages (Fig.5G-H, magenta puncta) suggesting that Lamp2 was transferred from proximal macrophages (Fig. 5 G-J). Importantly, a significant increase (2.3±1.8 in KO FB vs. 10.5±3.4 in KO FB with WT macrophages) in the number of autolysosomes (RFP$^+$/EGFP$^-$, red puncta) (Fig. 5L) was also observed, suggesting that LAMP2 was present on functional lysosomes, transferred from the WT macrophages, and could restore autophagic flux in *Lamp2* KO cells. In addition, Lamp2$^+$ lysosomes within *Lamp2 KO* mouse fibroblasts were observed (Fig.6E/F), suggesting the transfer of Lamp2 from macrophages to diseased cells.

Discussion

There is a pressing need to identify effective therapies for Danon Disease, a fatal condition associated with a severe cardioskeletal myopathy and multi-organ involvement for which there are presently no FDA-approved treatments. In this study, we show that single transplantation of pCCL-LAMP2B HSPC and WT mouse Sca-1$^+$ HSPCs into a young adult (2-month-old) LAMP2 KO mice was able to restore the expression of LAMP2 in cardiac myocytes (Fig. 2 and 3). It was also sufficient to rescue autophagic flux and decrease autophagic vacuole accumulation (Fig. 2), the hallmark of Danon disease, in the hearts of Danon mice (Fig.2). Most importantly, cardiac systolic function and behavior impairment both improved following de novo-expression of LAMP2 expression (Fig 2 and 4). These data suggest that the mechanism for this improvement involved the transfer of LAMP2$^+$ vesicles from both pCCL-LAMP2B and WT HSPC-donor-derived macrophages which reduced autophagic vacuoles in the heart tissues (Fig.4). The transfer of LAMP2$^+$ vesicles from HSPC-derived macrophages also resulted in a reduction in LC3-II levels in the heart tissues of HSPC-treated *Lamp2*KO mice compared to non-transplanted *Lamp2* KO mice (Fig.2) indicating rescue of autophagic flux. This mechanism is further supported by the macrophage-fibroblast coculture system which also demonstrated the rescue of autophagic flux (Fig. 5).

Hematopoietic stem and progenitor cell (HSPC) gene therapy has emerged as an efficient therapeutic technology for genetic disorders of the blood system but also for parenchymal diseases as they are able to travel and engraft into injured tissues [27, 28, 29, 30]. More recently, our group has evaluated this approach in a phase 1/2 human clinical trial for cystinosis (NCT03897361).[31] We also showed the beneficial impact of wildtype HSPCs transplantation on the cardiac function in Friedreich's ataxia[23]. One of the mechanisms by which modified HSPC leads to tissue preservation in cystinosis involves the transfer of lysosomes across TNTs[12]. These long membrane protrusions (~40 um) establish contact and enable cross-communication between macrophages and fibroblasts[14], and we observed a similar phenomenon in the context of Danon disease.

The mechanism by which loss of LAMP2 results in cardiac failure is not quite well understood. The LAMP2B isoform of LAMP2 is speculated to regulate macro-autophagic flux by mediating the fusion of lysosomes with autophagosomes [3,4,6-8,21]. Recent work by our group and others suggests impairment of LAMP2B mediated macro-autophagy plays an important role in the progression of cardiomyopathy in Danon patients[32]. Our recent *in vivo* study reported the prevention and reversal of severe cardiomyopathy in *Lmp2 KO* mouse model after intravenous injection of AAV9 (adeno-associated virus serotype 9)-HuLAMP2 complementary DNA (cDNA)[22]. Nonetheless, AAV9 therapy has specific limitations, including hepatotoxicity, limited uptake by the central nervous system, inability to use in patients with pre-existing antibodies, and unclear durability of gene expression. Due to limitations with current AAV9 vectors, more efficient ways to deliver LAMP2 to deficient cells may be needed. Here, we demonstrated that a single transplant of pCCL-LAMP2B mouse HSPCs into young adult Danon mice rescues multi-organ dysfunction including cardiac systolic function, neurobehavioral deficits, muscle weakness. The key advantage of exogenous HSPC transplantation is the capacity of these cells to permanently repopulate the bone marrow with LAMP2-expressing progenitor cells that can migrate from their niche to differentiate into phagocytic cell types within multiple end organs affected by Danon disease. Furthermore, autologous HSPCs have a less likely risk of rejection and are likely to exhibit sustained expression of LAMP2 over time. The other advantage is that HSPCs may even be able to transmigrate across the blood-brain barrier and engraft within the CNS as differentiated microglia [28, 33].

Several limitations of our study are worth noting. The LAMP2 mouse model does not develop some aspects of Danon disease seen in humans, such as cardiac hypertrophy or a reduction in ejection fraction despite having a strongly reproducible ultrastructural phenotype[19]. This is similar to many mouse models in which, despite the recapitulation of several aspects of the disease, the cardiac phenotype is not fully recapitulated, presumably due to inherent interspecies differences.

Furthermore, the lethal dose irradiation given during bone marrow transplantation caused severe diarrhea, dermatitis, and death; although this is unlikely to be an issue in patients, for whom chemotherapy will be used for myeloablation. In fact, it has been shown that chemotherapy agents for myeloablation such as busulfan do not typically cause cardiotoxicity and have a better impact on enhancing the repopulation of the CNS with bone marrow-derived microglia [34]. Further study is required to determine if transplantation improves the metabolic and physiologic function of other systems (skeletal muscle, spleen and eye), but is beyond the scope of the current study.

Conclusion

In summary, this study demonstrates that a single peripheral infusion of pCCL-LAMP2 treated HSPCs in a mouse model of Danon disease results in engraftment and differentiation of these cells into macrophages, and that their infiltration into heart, brain, and skeletal muscle induced *de novo* LAMP2 expression which improved end-organ dysfunction in several tissues. These improvements were likely

mediated by improved autophagic flux induced by *de novo* LAMP2 expression. Our findings may provide a new paradigm for the treatment of a wide assortment of lysosomal diseases due to dysfunctional transmembrane lysosomal proteins as well as autophagy-related disorders that collectively have a major impact on this family of rare and understudied multi-organ disorders.

Declarations

ACKNOWLEDGMENTS

We thank Dr. Joseph Hill (UT Southwestern) for generously providing us with the CAG-RFP-EGFP-LC3B mice. We thank UCSD CMM electron microscope facility for the preparation of EM slides. We thank Dr. Thomas Hnasko for generously sharing the open field maze recording system. We thank Dr. Marya Bengali in Cherqui's lab, Dr. Shelley Warlow and Lauren Faget in Dr.Hnasho's lab for assistance of open field maze test setting up. We thank Dr. Huanyou Wang for the spleen and bone marrow histology review. UCSD Neuroscience Microscopy Shared Facility was funded by Grant P30-NS047101. **Funding:** In Eric Adler's lab, this work was supported by the California Institute for Regenerative Medicine, CIRM (DISC2-11131), and H. S Lopez Family Foundation, founded by Czarina and Humberto S. Lopez. In Stephanie Cherqui's lab, this work was supported by the Cystinosis Research Foundation, the National Institute of Health (NIH) R01-NS108965, the California Institute of Regenerative Medicine (CIRM, CLIN-09230), and the Friedreich's ataxia Research Alliance (FARA).

AUTHOR CONTRIBUTIONS

Chao Chen, Sherin I. Hashem, Sylvia M. Evans, Stephanie Cherqui, Eric D. Adler: Conception and design; Chao Chen, Jay Sharma, Sherin I. Hashem, Ana M. Manso, Jose Roberto Cano Nigenda: Collection and assembly of data; Yusu Gu: cardiac catheterization and data analysis; Emily C. Gault, Angel Soto-Hermida: experiment assistance. Paul Saftig provided Lamp2 KO mice. Chao Chen and Sherin I. Hashem: data analysis/interpretation and manuscript writing/editing. Jason M. Duran, Paul Bushway, Jay Sharma, Ana M. Manso, Paul Saftig, Sylvia M. Evans, Stephanie Cherqui, Eric D. Adler: Manuscript editing.

ADDITIONAL INFOMATION

Stephanie Cherqui and Eric Adler are cofounders, shareholders, and a member of both the Scientific Board and Board of Directors of Papillon Therapeutics, Inc. Eric Adler is a shareholder of Rocket Pharmaceuticals and a consultant and shareholder of Lexeo therapeutics. Stephanie Cherqui serves as a consultant for AVROBIO and receives compensation for these services. Stephanie Cherqui also serves as

a member of the Scientific Review Board and Board of Trustees of the Cystinosis Research Foundation. The terms of this arrangement have been reviewed and approved by the University of California San Diego in accordance with its conflict-of-interest policies.

References

1. D'Souza R S, *et al.* Danon disease: clinical features, evaluation, and management. Circ Heart Fail **7**, 843–849 (2014).
2. Berko BA, Swift M. X-linked dilated cardiomyopathy. N Engl J Med **316**, 1186–1191 (1987).
3. Horvath J, *et al.* Identification of a novel LAMP2 mutation responsible for X-chromosomal dominant Danon disease. Neuropediatrics **34**, 270–273 (2003).
4. Balmer C, *et al.* Familial X-linked cardiomyopathy (Danon disease): diagnostic confirmation by mutation analysis of the LAMP2gene. Eur J Pediatr **164**, 509–514 (2005).
5. Syres K, *et al.* Successful treatment of the murine model of cystinosis using bone marrow cell transplantation. Blood **114**, 2542–2552 (2009).
6. Yeagy BA, Harrison F, Gubler MC, Koziol JA, Salomon DR, Cherqui S. Kidney preservation by bone marrow cell transplantation in hereditary nephropathy. Kidney Int **79**, 1198–1206 (2011).
7. Rocca CJ, *et al.* Treatment of Inherited Eye Defects by Systemic Hematopoietic Stem Cell Transplantation. Invest Ophthalmol Vis Sci **56**, 7214–7223 (2015).
8. Gaide Chevronnay HP, *et al.* Hematopoietic Stem Cells Transplantation Can Normalize Thyroid Function in a Cystinosis Mouse Model. Endocrinology **157**, 1363–1371 (2016).
9. Town M, *et al.* A novel gene encoding an integral membrane protein is mutated in nephropathic cystinosis. Nat Genet **18**, 319–324 (1998).
10. Kalatzis V, Cherqui S, Antignac C, Gasnier B. Cystinosin, the protein defective in cystinosis, is a H(+)-driven lysosomal cystine transporter. EMBO J **20**, 5940–5949 (2001).
11. Naphade S, *et al.* Brief reports: Lysosomal cross-correction by hematopoietic stem cell-derived macrophages via tunneling nanotubes. Stem Cells **33**, 301–309 (2015).
12. Goodman S, Naphade S, Khan M, Sharma J, Cherqui S. Macrophage polarization impacts tunneling nanotube formation and intercellular organelle trafficking. Sci Rep **9**, 14529 (2019).
13. Harrison F, Yeagy BA, Rocca CJ, Kohn DB, Salomon DR, Cherqui S. Hematopoietic stem cell gene therapy for the multisystemic lysosomal storage disorder cystinosis. Mol Ther **21**, 433–444 (2013).
14. Rafii MS, *et al.* A phase1 study of stereotactic gene delivery of AAV2-NGF for Alzheimer's disease. Alzheimers Dement **10**, 571–581 (2014).
15. Min YL, *et al.* Correction of Three Prominent Mutations in Mouse and Human Models of Duchenne Muscular Dystrophy by Single-Cut Genome Editing. Mol Ther **28**, 2044–2055 (2020).
16. Mullard A. Gene therapy community grapples with toxicity issues, as pipeline matures. Nat Rev Drug Discov **20**, 804–805 (2021).

17. Tanaka Y, *et al.* Accumulation of autophagic vacuoles and cardiomyopathy in LAMP-2-deficient mice. Nature **406**, 902–906 (2000).
18. Li L, Wang ZV, Hill JA, Lin F. New autophagy reporter mice reveal dynamics of proximal tubular autophagy. J Am Soc Nephrol **25**, 305–315 (2014).
19. Hashem SI, *et al.* Impaired mitophagy facilitates mitochondrial damage in Danon disease. J Mol Cell Cardiol **108**, 86–94 (2017).
20. Dull T, *et al.* A third-generation lentivirus vector with a conditional packaging system. J Virol **72**, 8463–8471 (1998).
21. Zychlinski D, *et al.* Physiological promoters reduce the genotoxic risk of integrating gene vectors. Mol Ther **16**, 718–725 (2008).
22. Manso AM, *et al.* Systemic AAV9.LAMP2B injection reverses metabolic and physiologic multiorgan dysfunction in a murine model of Danon disease. Sci Transl Med **12**, (2020).
23. Rocca CJ, *et al.* Transplantation of wild-type mouse hematopoietic stem and progenitor cells ameliorates deficits in a mouse model of Friedreich's ataxia. Sci Transl Med **9**, (2017).
24. Kustikova OS, Modlich U, Fehse B. Retroviral insertion site analysis in dominant haematopoietic clones. Methods Mol Biol **506**, 373–390 (2009).
25. Rothaug M, *et al.* LAMP-2 deficiency leads to hippocampal dysfunction but normal clearance of neuronal substrates of chaperone-mediated autophagy in a mouse model for Danon disease. Acta Neuropathol Commun **3**, 6 (2015).
26. Lin F, Wang ZV, Hill JA. Seeing is believing: dynamic changes in renal epithelial autophagy during injury and repair. Autophagy **10**, 691–693 (2014).
27. Cartier N, *et al.* Lentiviral hematopoietic cell gene therapy for X-linked adrenoleukodystrophy. Methods Enzymol **507**, 187–198 (2012).
28. Biffi A, *et al.* Lentiviral hematopoietic stem cell gene therapy benefits metachromatic leukodystrophy. Science **341**, 1233158 (2013).
29. Gentner B, *et al.* Extensive Metabolic Correction of Hurler Disease By Hematopoietic Stem Cell-Based Gene Therapy: Preliminary Results from a Phase I/II Trial. Blood **134**, (2019).
30. Visigalli I, *et al.* Gene therapy augments the efficacy of hematopoietic cell transplantation and fully corrects mucopolysaccharidosis type I phenotype in the mouse model. Blood **116**, 5130–5139 (2010).
31. Cherqui S. Hematopoietic Stem Cell Gene Therapy for Cystinosis: From Bench-to-Bedside. Cells **10**, (2021).
32. Taylor MRG, Adler ED. Danon Disease. In: *GeneReviews((R))* (eds Adam MP, *et al.*) (1993).
33. Sessa M, *et al.* Lentiviral haemopoietic stem-cell gene therapy in early-onset metachromatic leukodystrophy: an ad-hoc analysis of a non-randomised, open-label, phase 1/2 trial. Lancet **388**, 476–487 (2016).

34. Wilkinson FL, Sergijenko A, Langford-Smith KJ, Malinowska M, Wynn RF, Bigger BW. Busulfan conditioning enhances engraftment of hematopoietic donor-derived cells in the brain compared with irradiation. Mol Ther **21**, 868–876 (2013).

Figures

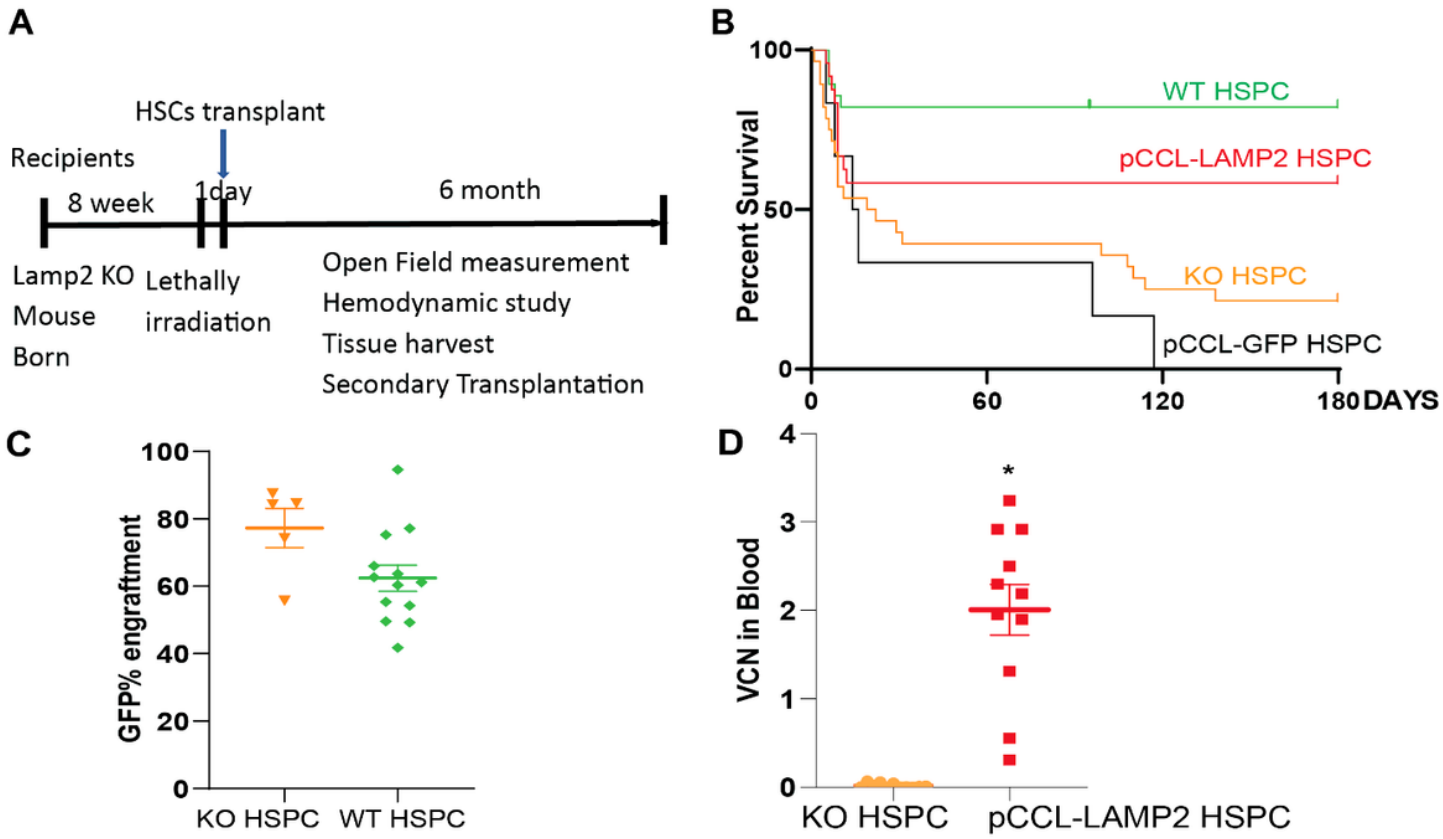

Figure 1

HSPC-transplantations, survival and Engraftment. **(A)** Schematic presentation of the in vivo experiments performed. **(B)** Survival assessment revealed that 60.87% of pCCL-LAMP2 HSPC group, 79.16% of mice WT-HSPC transplants survived 6 months compared to only 14.29% of mice in the KO-HSPC transplant group. Additionally, all the deaths that occurred in WT-HSPC transplantation group were within 2 weeks which caused by the irradiation. **(C)** Engraftment of donor bone marrow was assessed by flow cytometry 2 months post-transplant showing efficient engraftment in KO HSPC and WT HSPC groups. **(D)** VCN in blood. * $p<0.05$ vs. KO HSPC.

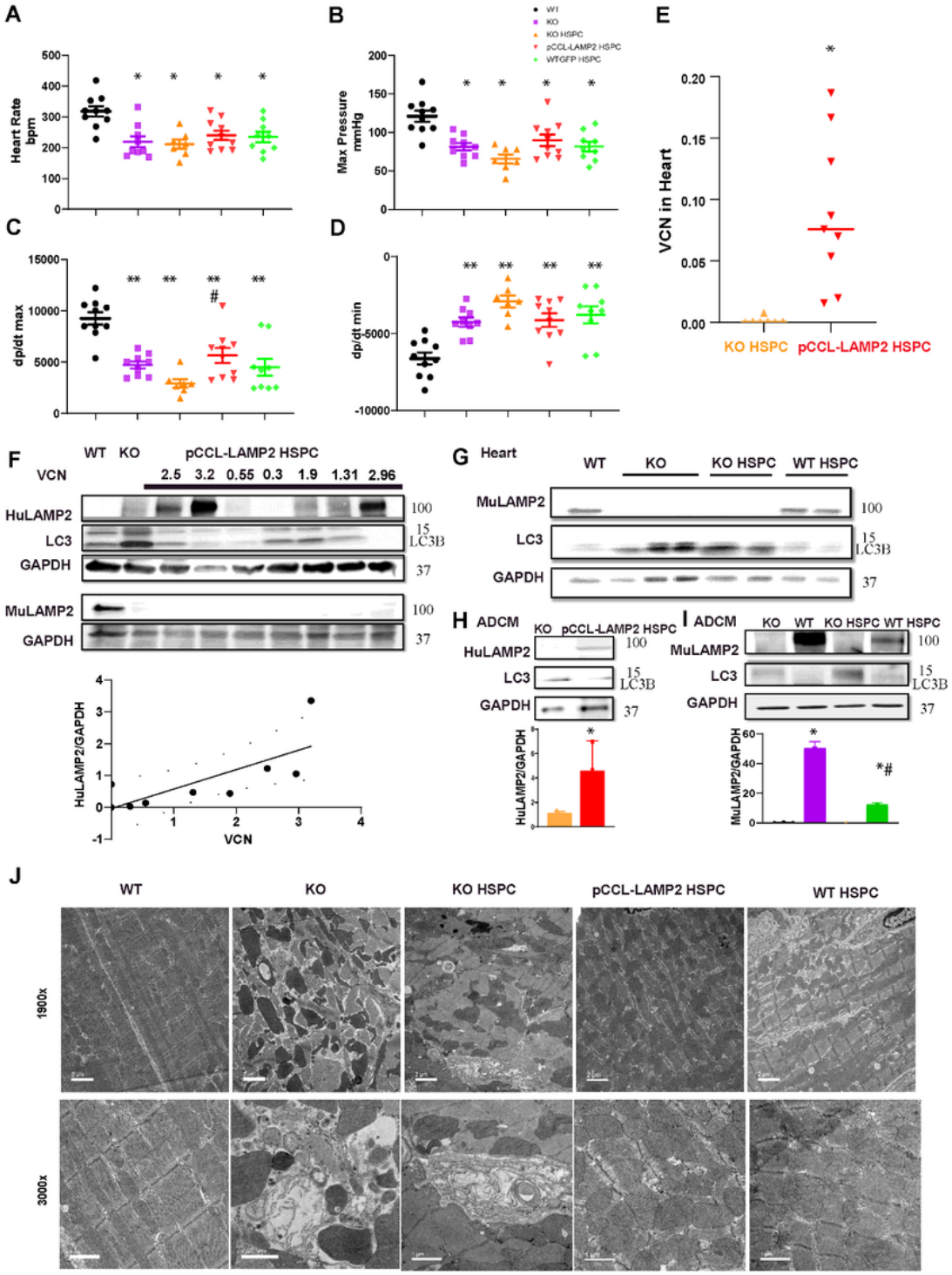

Figure 2

Gene-modified HSPC-transplanted Lamp2 KO mice improved the cardiac systolic function (dp/dt max)compared with Mock cell transplanted mice by hemodynamic measurement . (A) HR, heart rate; bpm, beats per minute; (B) Max pressure (The max pressure measured in the left ventricle); **(C)** dP/dt max (rate of rise of left ventricular pressure; contractility) and D) dP/dt min (rate of fall of left ventricular pressure; relaxation); **(E)** Heart VCN; **(F)** Representative HuLAMP2 WB of heart Tissue (Top) Quantification of WB

(Bottom); **(G)** Representative MuLAMP2 WB of heart Tissue; **(H)** Representative HuLAMP2 WB of Isolated Cardiomyocytes (ADCM); **(I)** Representative MuLAMP2 WB of ADCM. **(J)**Representative electron microscope (EM) images of heart. Scale bar=2 um. Wildtype(WT, n=8), Lamp2 KO(KO, n= 9), Lamp2 KO mouse transplanted with KO HSPC (KO HSPC, n=7), Lamp2 KO mouse transplanted with KO HSPC transduced with pCCL-LAMP2 (pCCL-LAMP2 HSPC, n=9), Lamp2 KO mouse transplanted with WTGFP HSPC(WT HSPC, n=9)(One way ANOVA , * $p<0.05$ or** $p<0.01$ vs. WT, # $p<0.05$ vs. KO HSPC, $ $p<0.05$ vs. KO).

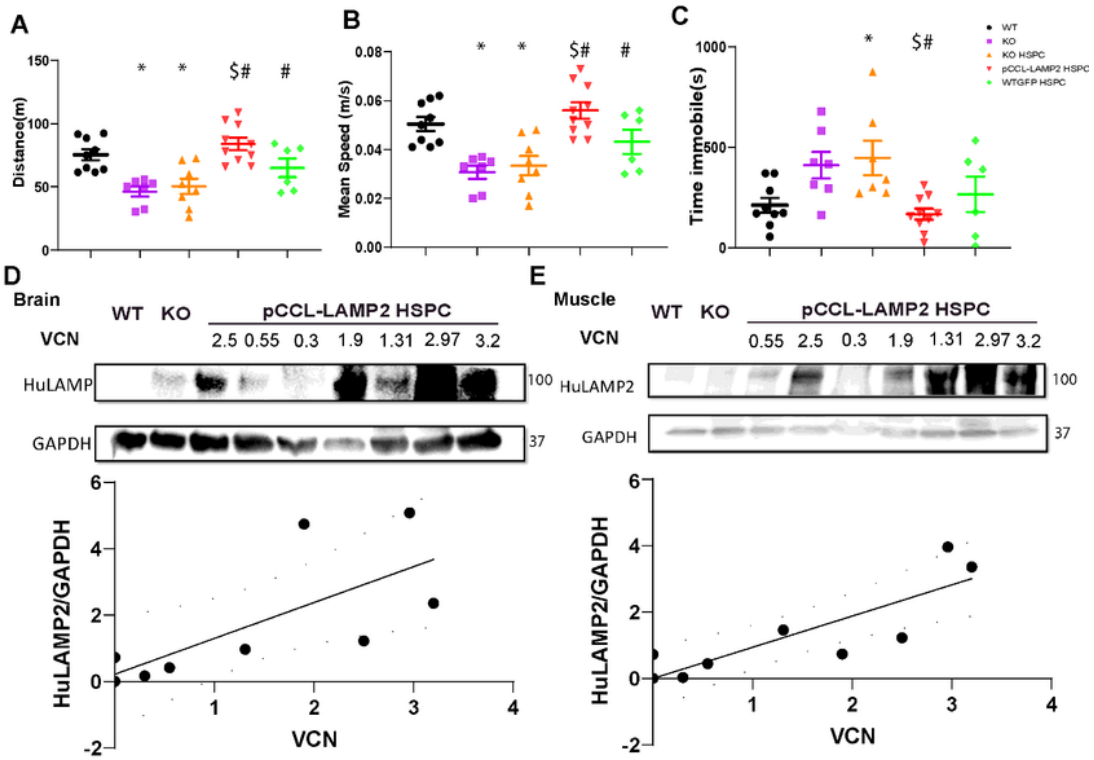

Figure 3

Gene-modified HSPC-transplanted *Lamp2* KO mice improved the abnormal behavior of *Lamp2* KO mice in the Open Field Maze study. **(A)** Path length during exploration of a novel environment. **(B)** Mean walk speed during exploration of a novel environment. **(C)** The immobile time during exploration of a novel environment. **(D)** Representative HuLAMP2 WB of Brain Tissue(Top) Quantification of WB(Bottom); **(E)** Representative HuLAMP2 WB of Brain and Muscle Tissue(Top) Quantification of WB(Bottom); Wildtype

(WT, n=9), Lamp2 KO (KO, n= 7), Lamp2 KO mouse transplanted with KO HSPC (KO HSPC, n=8), Lamp2 KO mouse transplanted with KO HSPC transduced with pCCL-LAMP2 (pCCL-LAMP2 HSPC, n=10), Lamp2 KO mouse transplanted with WTGFP HSPC (WT HSPC, n=9) (One way ANOVA , * p<0.05 or**p<0.01 vs. WT, # p<0.05 vs. KO HSPC, $ p<0.05 vs. KO).

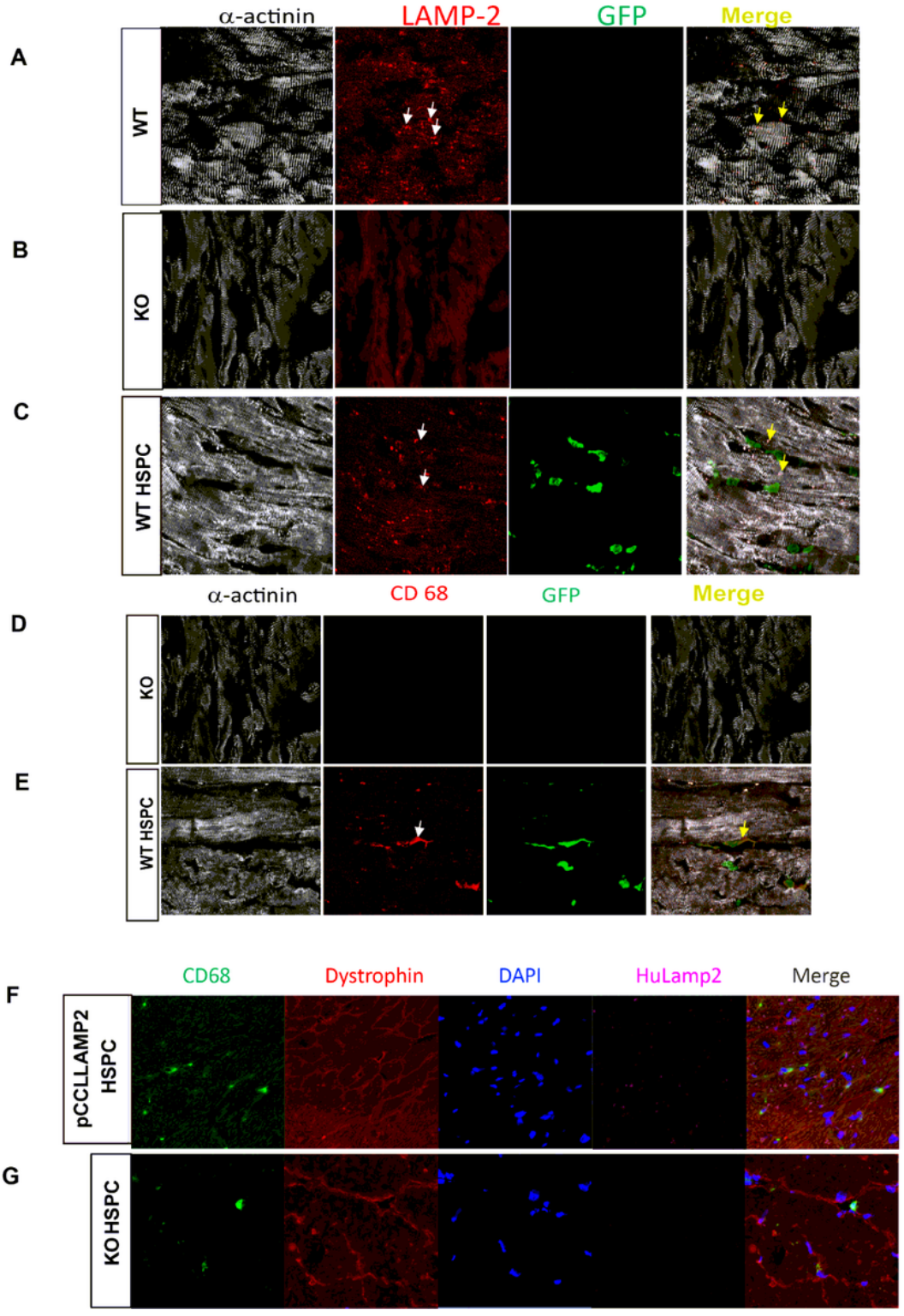

Figure 4

LAMP2 localized in cardiomyocytes in both WT HSPC and the gene-modified HSPC transplanted mouse. A to C) Representative Mouse LAMP2 immunofluorescence staining of heart sections from WT**(A)**, KO**(B)** and Lamp2 KO mice transplanted with WTGFP HSPC**(C); (D and E)**) The GFP^+ cell is macrophages stained by CD68. Arrow demonstrated the colocalized GFP^+ and $CD68^+$ cell. **(F and G)** Representative human LAMP2 immunofluorescence staining of heart sections from KOHSPC and Dystrophin (Dys) and a-actinin were used to mark and localize cardiac myocytes. DAPI, 4',6-diamidino-2-phenylin. Yellow arrows pointed to the LAMP2 in cardiomyocytes.

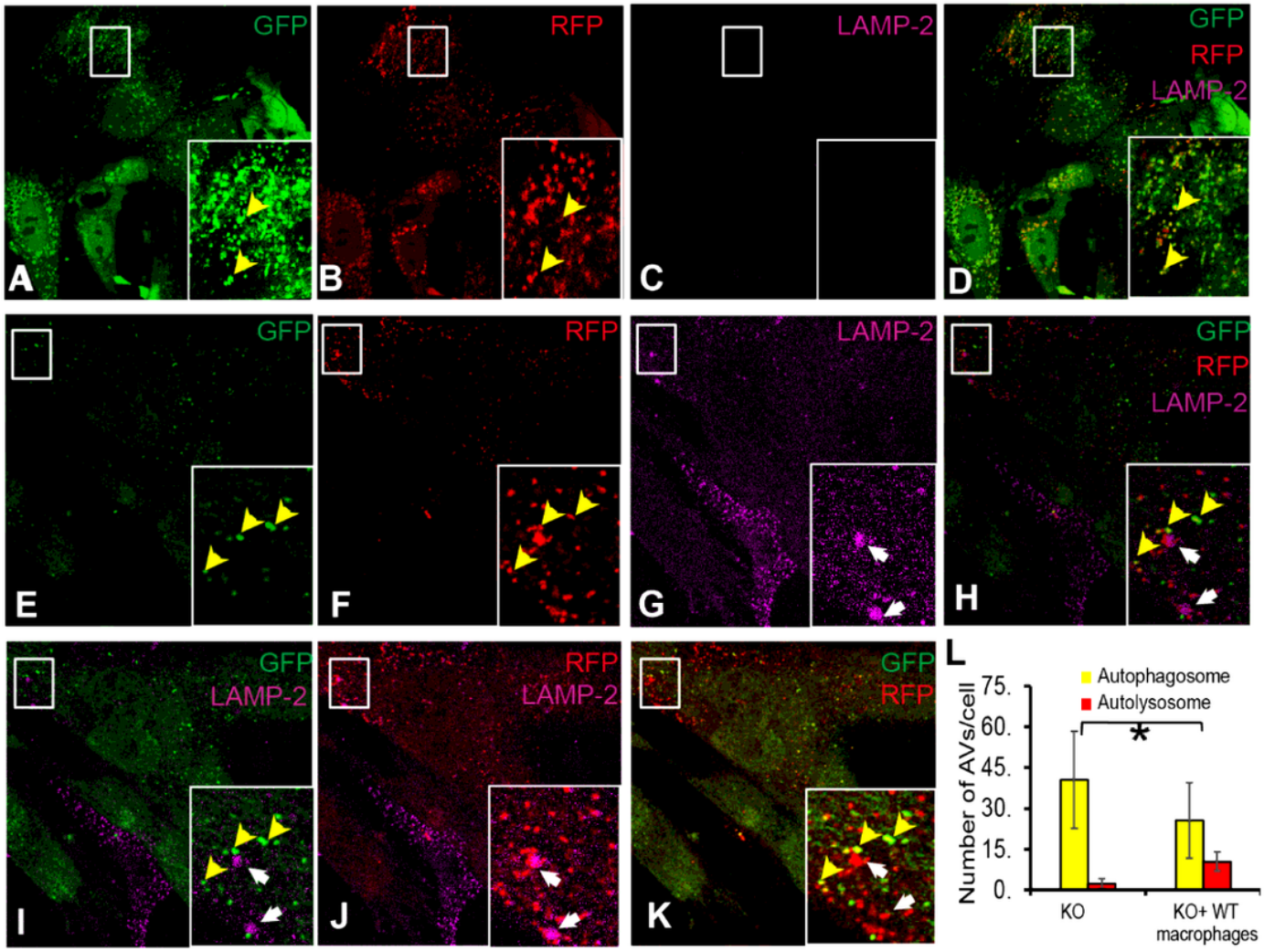

Figure 5

LAMP2-positive lysosomes from WT macrophages transfer into and rescue autophagic flux in *Lamp2* KO/CAG-RFP-EGFP-LC3B mouse fibroblasts located at close proximity in vitro. (A-D) Representative

confocal images of *Lamp2* KO/CAG-RFP-EGFP-LC3B (i.e. reporter positive: R+) fibroblasts (FB) cultured without WT macrophages(M) showing lack of *Lamp2* expression, increased accumulation of autophagosomes (GFP+RFP=yellow vesicles), and lack of autolysosomes (RFP only vesicles). **(A)** GFP (green), **(B)** RFP (red), **(C)** *Lamp2* (magenta), and **(D)** merge of the 3 channels. **(E-K)** Representative confocal images of *Lamp2* KO/CAG-RFP-EGFP-LC3B fibroblasts co-cultured with WT macrophages showed the presence of LAMP2 vesicles in fibroblasts located in contact with WT macrophages, reduction in the number of autophagic vacuoles (AVs), as well as the presence of autolysosomes (RFP only vesicles). **(E)** GFP (green), **(F)** RFP (red), **(G)** LAMP2 (magenta), **(H)** merge of the 3 channels, **(I)** merge of GFP and LAMP2, **(J)** merge of RFP and LAMP2, **(K)** merge of GFP and RFP. Yellow arrows: autophagosomes; white arrows: autolysosomes. **(L)** Quantification of AVs (autophagosomes i.e. yellow vesicles; autolysosomes i.e. red-only vesicles) in *Lamp2* KO/CAG-RFP-EGFP-LC3B cultured with or without WT macrophages. * $p < 0.05$, n=3. Student's t-test. Data presented as mean ± SD.

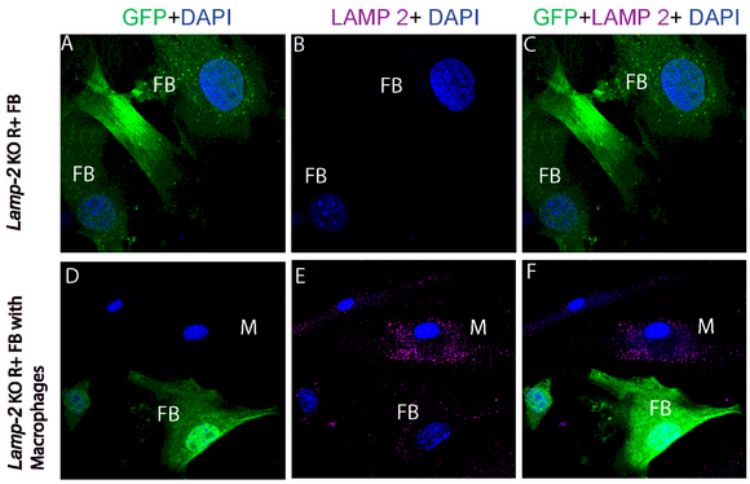

Figure 6

LAMP2-positive lysosomes from WT macrophages transfer into Lamp2 KO R+ mouse fibroblasts located at proximity in vitro. Representative confocal images of Lamp2 KO/CAG-RFP-EGFP-LC3B (i.e. reporter positive: R+) fibroblasts (FB) cultured without WT macrophages (M) showing lack of Lamp2 expression. Representative confocal images of Lamp2 KO/CAG-RFP-EGFP-LC3B fibroblasts co-cultured with WT macrophages showing the presence of LAMP2 vesicles in fibroblasts located in contact with WT

macrophages. The reporter line is used to differentiate in culture between the Lamp2 KO fibroblasts (reporter positive: R+) and macrophages (reporter negative). GFP: green, DAPI nuclear stain: blue, LAMP2: magenta, M: macrophage, FB: Fibroblast.

Supplementary Files

This is a list of supplementary files associated with this preprint. Click to download.

- SUPPLEMENTALMATERIALS.docx